

# Performance evaluation of photonic crystal ring resonators based optical channel add-drop filters with the aid of whispering gallery modes and their $Q$ -factor

Alireza Tavousi · Mohammad Ali Mansouri-Birjandi

Received: 7 May 2014 / Accepted: 4 September 2014 / Published online: 17 September 2014  
© Springer Science+Business Media New York 2014

**Abstract** As a basic type of linear defects, the PhC ring resonators are considered the most fascinating elements to be used in photonics integrated circuits for applications such as dense wavelength division multiplexing and Optical filtering that are among the most important components of the telecommunication systems. This article proposes two different optical channel add-drop filters (CDFs) based on rod-type two-dimensional square-lattice all-circular photonic crystal ring resonator. In the studied ring-type PhC cavity, there are some modes that are analogous to whispering gallery (WG) modes. For the proposed all-circular PhC ring resonator, the WG-like mode with the azimuthal mode number  $m = 10$ , couples out from cavity to the drop waveguide. Although because of the absence of perfectly circular symmetry, these WG-like modes are not exactly degenerate but they form a close doublet. The normalized frequencies ( $a/\lambda$ ) of the doublets of  $m = 10$  are  $a/\lambda = 0.3684$ , and  $0.3645$  and their  $Q$ -factors are 1050, 866 respectively. By selecting appropriate coupling distance between the PhC ring resonator and side-coupled  $W_1$  waveguide, the CDFs are formed. For a TM polarized Gaussian source, the drop efficiency of both filters is more than 99.8% in the 1.535–1.625  $\mu\text{m}$  wavelength interval. The photonic bandgap and the WG-like modes of the PhC ring resonator are calculated using the PWE method, and the  $Q$ -factor of modes and the transmission spectra of CDFs are calculated using 2D-FDTD method.

**Keywords** Optical channel add-drop filter · Finite-difference time-domain · Plane wave expansion method · Photonic crystal · Ring resonator · Whispering gallery modes

---

A. Tavousi · M. A. Mansouri-Birjandi (✉)  
Faculty of Electrical and Computer Engineering, University of Sistan and Baluchestan,  
P.O. Box 98164-161, Zahedan, Iran  
e-mail: mansouri@ece.usb.ac.ir

A. Tavousi  
e-mail: tavousi@tabrizu.ac.ir

## 1 Introduction

Hybrid optoelectronic elements work only up to few hundreds of gigabit per second (Yariv and Yeh 2006). To go beyond that speed, purely all-optical elements e.g. sources, detectors, waveguides and etc., are required (Gibbs 1985). The main goal in designing pure all-optical devices is to create all-optical integrated circuits and all-optical networks without any electrical parts. Presently photonic crystals (PhCs) are the best platforms for this goal (Sakoda 2005). As the main advantage of the PhC, one can mention the complete integration of optical elements on fully optical chips which operate at much higher frequencies and require less power than electronic chips (Bush et al. 2004).

The field of PhCs is growing rapidly due to their new electromagnetic wave characteristics, which add extraordinary abilities to them e.g. controlling, modifying, and harvesting the flow of light (Joannopoulos et al. 2008). The behavior of electromagnetic wave with a certain energy and frequency propagating in a PhC is intuitively understood by comparing it to that of electrons in solid-state materials. The electrons passing through a lattice of the atoms interact with a periodic potential. This results in the formation of allowed and forbidden energy states of electrons. The propagating light in a PhC interacts with the periodic modulation of dielectric constant(s), which results in the formation of allowed and forbidden bands in optical wavelengths (Joannopoulos et al. 2008; Sakoda 2005). Therefore PhCs prohibit any propagation of light with wavelengths in the forbidden bands, i.e., the photonic bandgaps (PBGs), while allowing other wavelengths to propagate freely. In state of energies which the propagation of photons regardless of their path or polarization is not allowed, a complete photonic band gap is formed (Inoue and Ohtaka 2004). By adjusting the bandgap of each PhC structure through controlling the structure parameters such as lattice and dielectric constants or the radius of the elements, one can control the transmittance and reflectance wavelengths interval (Joannopoulos et al. 2008).

One can design PhCs in different shapes and with different optical bandgap characteristics (Sakoda 2005). The simplest way to tune the wavelength interval is based on a mixture of defects such as various number of point and line defects. Parameters like the location and the situation of defects are extremely important parameters to control and direct the transmitted light beam (Guo and Albin 2003).

In recent years many PhC based optical elements, theoretically and experimentally have been shown possible. These elements include channel (Olivier et al. 2002) and slab waveguides (Janfaza and Mansouri-Birjandi 2013; Vlasov et al. 2005), polarization beam and power splitters (Yu et al. 2011; Chung and Yoon 2003), multiplexers and de-multiplexers (Ghaffari et al. 2008; Ghasemi 2013; Manzacca et al. 2007), channel drop (add-drop) filters (CADF) (Djavid and Abrishamian 2012; Tavousi et al. 2012), multi layered tunable optical thin film fabry-perot filter (Ghasemi 2013), logic gates (Ghadrdan and Mansouri-Birjandi 2013) and so on.

Special limitations of these devices are unsatisfactory quality factor ( $Q$ ) (Lalanne et al. 2004) and efficiency of the needed wavelength and other figure-of-merit parameters. To compensate these shortages and enhancing them, PhC resonant cavities are used which can improve the interaction of light (Rafizadeh et al. 1997).

Optical filtering elements are among the most important components of the telecommunication systems. They separate desired wavelengths from the signal by uniquely designed central wavelength and bandwidth. They are able to selectively transmit light with a specific wavelength window and route or block the remainders (Qiang et al. 2007). One can design tunable filters so they pass signals in some frequency bands, and attenuate them in others.

Filters are classified according to their frequency domain properties. Customary ones are low-pass, high-pass, band-pass, band-stop, all-pass and notch filters (Li 2010; Monifi et al. 2008; Chu et al. 2006; Suh and Fan 2004). Based on the circular PhC ring resonator (Robinson and Nakkeeran 2011, 2012) and to meet DWDM filtering needs with high dropping efficiency, high coupling efficiency and tuning ability (Xu et al. 2011), in this work we developed a compact integrated *channel-drop* optical filter with three and four output ports. The novelty of this research consists in the optimized design of the all-circular PhC ring resonator itself and for the first time we have investigated the properties of the whispering gallery (WG)-like modes and their quality factors for this type of all-circular PhC ring resonator (Qiang et al. 2007; Guo and Albin 2003). The quality factor ( $Q$ ) for each mode is calculated and the mode with highest  $Q$ -factor which can couple out to the designed  $W_1$  waveguide is clearly identified and confirmed through simulations.

In the next sections, the simulation results authenticate that the proposed structure has a relatively high quality factor and is suitable for photonic crystal integrated circuit design.

## 2 Methods of numerical simulation

To study, analyze and extracting the properties of PhC devices, one needs to employ some numerical methods. The plane wave expansion method (PWE) and multiple scattering theories are the interesting ones at frequency domain (Johnson and Joannopoulos 2001). Although the PWE method is superior in calculating the band diagrams and modal field patterns but it suffers from a few disadvantages. The structure must be periodic and infinite in all three dimensions, and when simulating frequency dependent materials, convergence problems are encountered (Stieler 2008). In the case where the pure periodicity of the crystal is broken, or there is a defect, the so called supercell approach has to be used, which is computationally heavy as the number of plane waves used in the expansion increases (Joannopoulos et al. 2008).

Finite Difference Time Domain (FDTD) is another effective method for analysis of PhC structures. FDTD provides EM field variations in space with respect to time. In the general procedures, finite differences are used to approximate Maxwell's curl equations in real space and appropriate boundary conditions are imposed in order to simulate finite or infinite structures. Then the response of the structure to the EM waves in time domain can be obtained by time-marching the fields. This method was introduced by K. Yee in 1966 (Yee 1966). The transmission and reflection spectra of finite structures can be evaluated easily and the wave propagation through the medium can be observed in time. This method may be more favorable in direct comparison with experiments. In addition, frequency dependence and loss can be included in this method. Although there are some drawbacks mentioned for the accuracy of the conventional FDTD codes in the computation of the field patterns located near high- $Q$  WGM resonances, but resonances with  $Q$ -factors up to  $10^3$  are still detectable with FDTD (Boriskin et al. 2008). Band diagram calculations are tedious with the FDTD as the selection of the initial excitation field is important to excite all possible modes, e.g. the detection points shouldn't be placed at a high symmetry point (Joannopoulos et al. 2008). Various techniques have been proposed to improve the performance of FDTD solvers (Liu and Sarris 2006; Shlager and Schneider 1995). As a result, reasonable agreement between the FDTD and the experiment is often reported (Sakai and Baba 1999).

Unless otherwise noted, all the discussions here are based on the 2D square rod-type lattice. To simulate the behavior of a silicon-on-insulator (SOI) PhC structure operating at telecommunication wavelengths, the dielectric constant of the silicon (Si) rods is  $\epsilon_h = 12$  and surrounding background is air. Due to large refractive index difference with air, silicon

material provides a wide PBG (Meade et al. 1997). Although the real SOI structure would in practice require 3D numerical analysis (3D FDTD) which is typically highly time and memory consuming, the 2D approach is used since it gives a general indication of the expected 3D behavior (Robinson and Nakkeeran 2013).

In general, dielectric-rod-type PhC waveguides (pillar) can be easily designed to operate in single mode while air-hole-type PhC waveguides tend to function in multimode regime without any other structural modifications or optimizations. Thus, for simplicity, we first consider the 2D array of rods within a low-index slab, i.e., dielectric-rod-type PhC waveguides. While the rods are best suited to TM light ( $\sim E$  parallel to the rods), and the holes are best suited to TE light ( $\sim E$  running around the holes) (Joannopoulos et al. 2008).

The quality factor of WG-like modes and the power transmission spectra have been calculated using FDTD numerical method with perfectly matched layer (PML) absorbing boundary conditions (ABC) and PhC ring resonator WG-like modes along PhC band structure were calculated by mean of PWE method.

The FDTD mesh size and time step are  $\Delta x = \Delta y = a/64$  and  $\Delta t = \Delta x/2c$  ( $c$  is speed of light in free space) respectively. To obtain the time response of the filter, a pulse excitation which consists of a Gaussian envelope function multiplying a sinusoidal carrier with  $2^{18}$  time steps is used at the input waveguides which is adequate to excite the fundamental waveguide mode and PhC ring resonator evanescent modes.

Since we desire the frequency response of the filter in order to obtain the spectral characteristics of the structure, we perform a frequency analysis which is based on discrete Fourier transform (DFT) algorithm on the time response of the filter. Our DFT analysis is calculated for  $\Delta\lambda = 1.576 \mu\text{m}$  with center wavelength of  $\lambda = 1.576 \mu\text{m}$ . All of the power transmission spectral responses are calculated as the relation of transmitted power versus wavelength and are normalized to the incident light. A continuous wave (CW) Gaussian excitation source is used to simulate the filter's behavior in a single wavelength such on or off-resonance and an impulse Gaussian excitation with center wavelength of  $\lambda = 1.576 \mu\text{m}$  is used to find the  $Q$ -factor of the PhC ring resonator whispering gallery modes.

### 3 Structure design, optimization and $Q$ -factor calculation

The photonic bandgap of the PhC structure is shown in Fig. 1 which is calculated through PWE method and TM polarized plane wave for a perfect lattice with filling factor of  $r/a = 0.17$ .

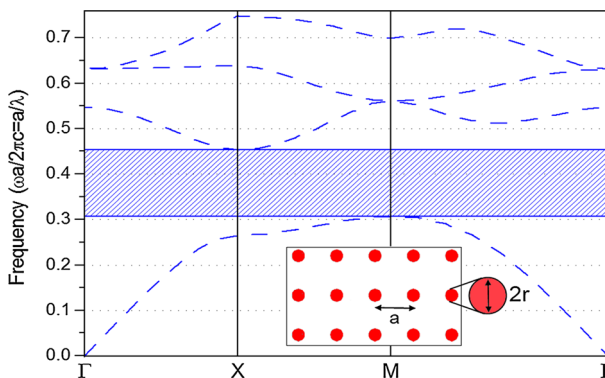


**Fig. 1** Formation of photonic bandgap in the first two bands of a rod-type square-lattice PhC structure with filling factor of  $r/a = 0.17$ . This is calculated through PWE method using TM polarized incident plane wave

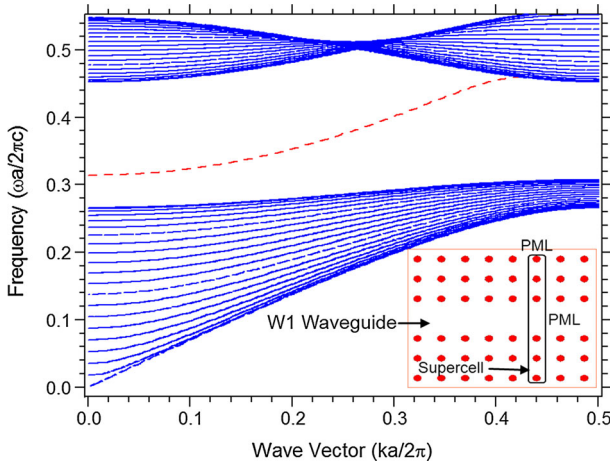


**Fig. 2** The  $W_1$  waveguide dispersion curve calculated through PWE method. This waveguide supports single mode propagation of TM polarized light

The horizontal 'X' axis links the points of the first Brillion zone which is the smallest periodical space of PhC lattice and the vertical 'Z' axis represents the normalized frequency  $\omega a/2\pi c = a/\lambda$  where ' $\omega$ ' is the angular frequency, ' $a$ ' is a constant for distance between centers of two adjacent rods, ' $c$ ' is the speed of light in the free space and ' $\lambda$ ' is the vacuum wavelength.

For the TM polarized incident plane wave, the PBG is formed in the first two bands of this figure. Since the PBG frequency range is  $0.3076 \leq a/\lambda \leq 0.4526$  and the width of normalized band gap is  $\Delta\omega a/2\pi c \approx 0.145$ , one can easily find the wavelength interval that is located within the conventional C ( $1.53 \sim 1.565 \mu\text{m}$ ) and L ( $1.565 \sim 1.625 \mu\text{m}$ ) bands of optical telecommunications.

Since the guidance of light toward the ring resonator happens through a  $W_1$  waveguide, finding its dispersion characteristics is vital. To obtain this curve a supercell of rods with the size  $7a \times 1a$  (the inset of Fig. 2) is used. For  $W_1$  waveguide, the ability of mode guidance is the most important characteristic in the dispersion curve. In Fig. 2, we found that this waveguide is able to guide in a single mode for an incident TM polarized light in the symmetry point direction  $k = \Gamma$ .

### 3.1 Photonic crystal ring resonator

As a basic type of linear defects, the PhC ring resonators are considered the most fascinating elements to be used in photonics integrated circuits for applications such as dense wavelength division multiplexing (DWDM). The size of this closed loop quasi-circular waveguide is determined by the desired wavelength. One can mention higher compactness and hence better functionality as an advantage for them over other conventional ring resonator based optical elements (Qiang et al. 2007). In comparison with point or linear defect, PhC ring resonators are more scalable in size due to various design parameters such as radius of the ring resonator and even the radius and number of surrounding and scattering rods. Even the reactive index of each single rod or the whole structure is tunable and can lead to better flexibility in the structure design. These are important key attributes for PhC ring resonators

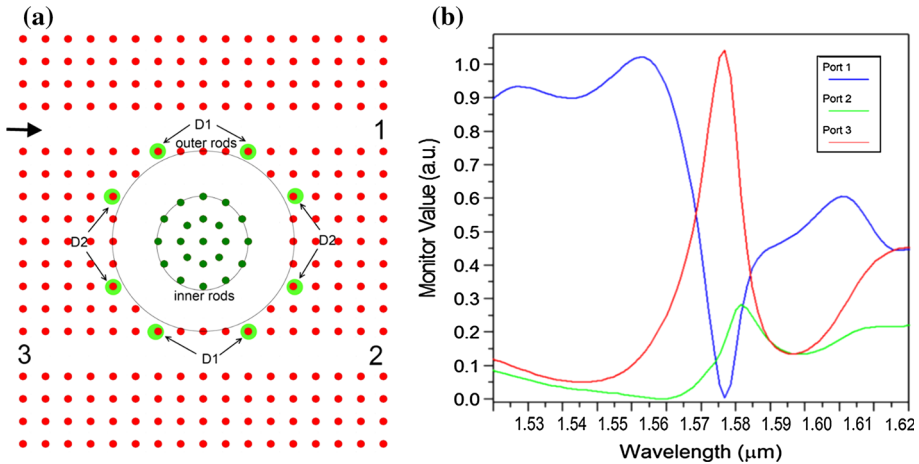


**Fig. 3** **a** The add-drop filter (four-port CDF) with circular lattice inner rods. The location of  $D_1$  and  $D_2$  rods are optimized through CW FDTD and no scattering rods is introduced within the structure. **b** The transmission spectra of this add-drop filter. Since Port-1 has a 99.8% drop efficiency but the symmetry of its spectrum is not desirable

to be used as building blocks for large scale integration. (Robinson and Nakkeeran 2011; Ghaffari et al. 2008a).

When the light with an appropriate wavelength is launched to the input (bus) of a waveguide that is side-coupled to one or more PhC ring resonators, it will couple to the ring through evanescent coupling. Due to several round-trips and the constructive interference phenomena, the intensity builds up for special wavelengths and resonance happens. At resonance, also a much higher intensity exists in the ring. These intensities are evanescent and exponentially decay out of the ring (Xiao et al. 2008). Since only some wavelengths resonate within the ring, it somehow functions as a wavelength selective filter (Rafizadeh et al. 1997).

The four and three-port channel drop filters are within the fundamental building blocks for optical modulators and switching elements that are needed for photonic integrated circuits and optical communication systems (Villeneuve et al. 1996). In Fig. 3a we propose our first design of an add-drop filter (four-port CDF). The inner rods are shaped in a circular lattice and none scattering rods is introduced to the structure. The two ends of the bus waveguide which carry the incident light toward the ring are named as the input and Port-1. The coupling length of the bus waveguide to ring is five times of the lattice constant ( $5a$ ) in the lateral 'X' direction and one times of the lattice constant ( $1a$ ) in the vertical 'Z' direction. The dropping waveguide is the other one and its endings are labeled as Port-3 and Port-4 respectively.

The power transmission spectra for this CDF are shown in Fig. 3b. In order to improve output spectra with enough symmetry, one must perform extensive numerical simulations. These simulations are performed through continues wave (CW) FDTD method. We found that changing the location, the size and even the dielectric constant of  $D_1$  and  $D_2$  rods are very effective choices to affect the output spectra. But since we like to keep the design as simple as possible in order of using fewer masks in manufacturing, we ignored the choices of changing the dielectric constant and rod size and only studied the location parameter. Our first step is to shape outer rods of the ring as more circular as possible. To do this, the defects labeled  $D_1$  and  $D_2$  are moved. The  $D_1$  defects are moved about 4% from their post in toward vertical 'Z' axis and  $D_2$  defects are moved along the lateral 'X' axis to 4% of their primary location.

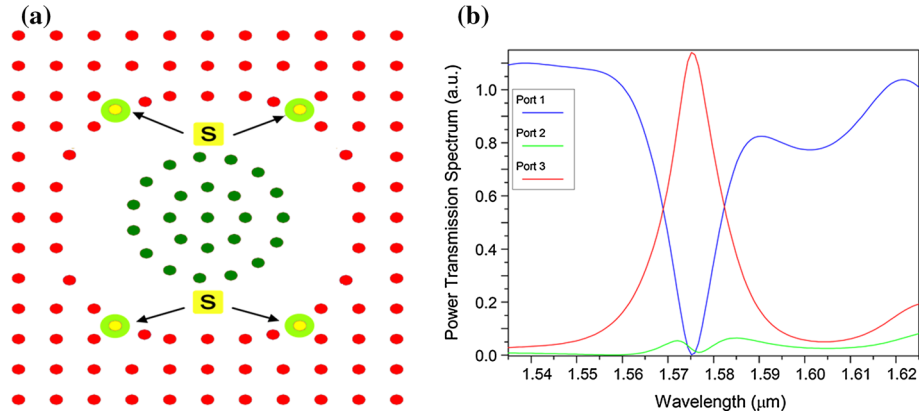


**Fig. 4** **a** Four scatterer rods labeled as (S) are added to the corners of the PhC ring resonator to improve the performance of the ring. **b** Transmission spectral response of the four-port CDF when the four scattering rods are introduced and their location is optimized via CW FDTD. The Port-1 now has a better symmetry and its dropping efficiency is around 100 %

Due to rather big radius of this ring (Robinson and Nakkeeran 2011; Qiang et al. 2007; Villeneuve et al. 1996), at resonant, filter operates as a backward-dropping one and Port-3 is the main output. Since the PBGs corresponding wavelength interval is in the conventional C and L bands of optical telecommunications, our filter also will work in that window. Although this CDF can operate in a wide window and Port-1 has a drop efficiency of about 99.8 % but the power transmission spectra are not symmetric enough. This is counted as a disadvantage for this CDF.

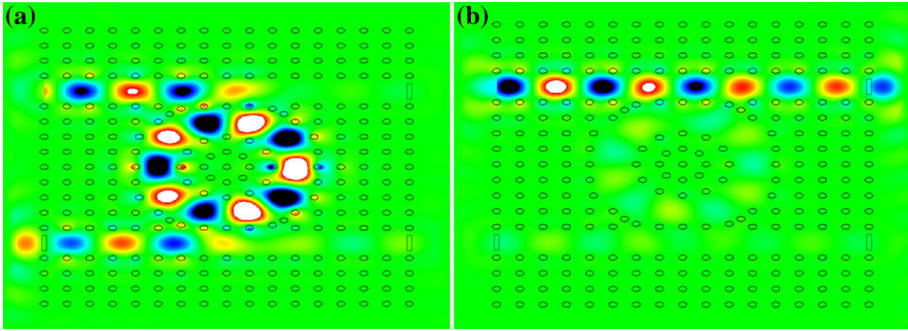
According to other optimization works done for of the output spectra in this types of the rings (Robinson and Nakkeeran 2013; Qiang et al. 2007; Darki 2010), adding scattering rods to the structure would be a nice choice. Thus we introduced four extra rods as scattering ones near  $D_1$  on the center of the imaginary square made by its four adjacent rods. These scattering rods which are indicated with label (S) in Fig. 4a, are the same as other rods in shape, radius and dielectric constant. These rods act like reflectors, so they will reduce back-reflections from their corresponding corners. Extensive optimizations were performed and ultimately, the optimized locations of this 12 point-defects ( $D_1$ ,  $D_2$  and S) within PhC ring resonator structure in two separate individual steps were found.

Figure 4b demonstrates the transmission spectra of the optimized single ring four-port CDF. These spectra are depicted for the wavelengths range 1.535–1.625 μm and are normalized to the incident light. Due to several round-trips of light in the ring, the constructive interferences happen and the light intensity builds up and become slightly more than unity. The dropping efficiency for the third output channel of this CDF is close to 100 % and its peak of resonance is located near  $\lambda = 1.576 \mu\text{m}$ .

Figure 5a, b demonstrates a single shot of the CW FDTD numerical simulation results in the time domain for the peak of resonance wavelength  $\lambda = 1.576 \mu\text{m}$  and an arbitrary non-resonant wavelength e.g.  $\lambda = 1.54 \mu\text{m}$ , respectively. The full-width-half-maximum (FWHM) bandwidth of this filter from  $\lambda = 1.568 \sim 1.583 \mu\text{m}$  is calculated about 15nm.

At resonance condition which happens for the peak of the transmission spectra, the electric field component inside the ring resonator completely couples to the drop waveguide and reaches to Port-3. Since the output of Port-1 and Port-2 is very little and hence can be ignored, we can reach a near critical coupling condition (critical coupling condition is the





**Fig. 5** The CW FDTD numerical simulation results for the four-port channel drop filter with optimized scattering rods when: **a** ring is on-resonance with  $\lambda = 1.576 \mu\text{m}$  so a WG-like mode with azimuthal mode number  $m = 10$  is formed **b** ring is off-resonance with  $\lambda = 1.54 \mu\text{m}$

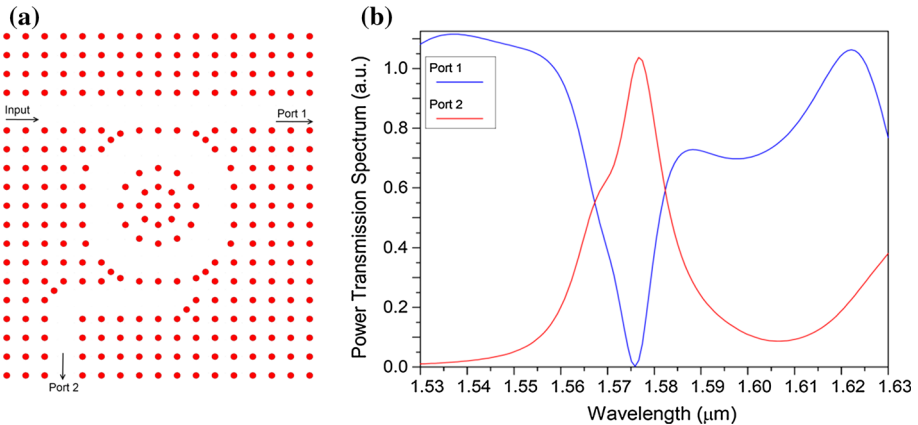


**Fig. 6** **a** The three-port CDF formed by terminating port-2 of Fig. 3a and introducing the  $90^\circ$  bend at the other output port. **b** Transmission spectral response of the three-port CDF with  $90^\circ$  bend in output port. The Port-1 has an acceptable symmetry and its dropping efficiency is around 100 %

condition where the output of ports except the drop one, is zero). One can see that the electric field component inside the ring resonator has formed a WG-like mode with azimuthal mode number  $m = 10$ . For the off resonance case of Fig. 5b where the incident wavelength is  $\lambda = 1.54 \mu\text{m}$ , light doesn't couple with the ring and goes away from ring via Port-1.

Terminating the Port-2 of previous CDF, will form a more simpler CDF which can have other applications rather than just add and dropping the wavelengths, e.g. multiplexing, de-multiplexing and even all-optical analog to digital conversion. Also a bend with  $90^\circ$  is introduced in the drop waveguide of Fig. 6a. By adding a reflector rod, the bend is designed such that its efficiency is 100 % and there is no attenuation of light (Espinola et al. 2001; Stoffer et al. 2000). Also the coupling length parameter between the bus waveguide and all-circular PhC ring resonator is the same as the previous CDF.

Figure 6b depicts the single-ring three-port CDF normalized transmission spectra in the wavelengths interval  $1.535\text{--}1.625 \mu\text{m}$ . The Port-2 performs the dropping job in resonance condition. Since the PBG and the ring structure have not changed, the filter's wavelength performance window is the same as before. The CDF dropping efficiency for the second output



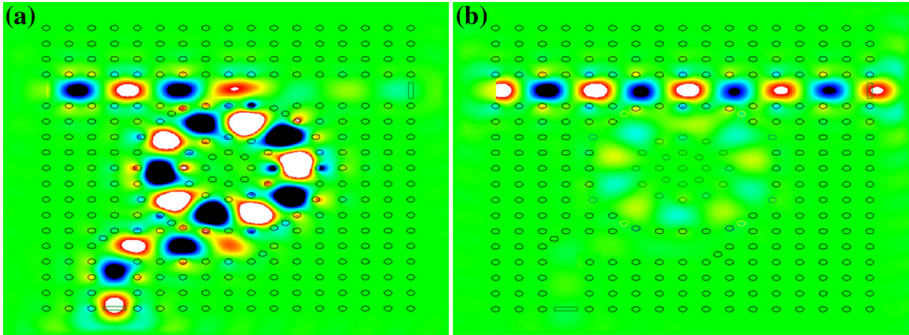


**Fig. 7** The CW FDTD numerical simulation results for the three-port channel drop filter with optimized 90° bend when: **a** ring is on-resonance with  $\lambda = 1.576 \mu\text{m}$  so a WG-like mode with azimuthal mode number  $m = 10$  is formed **b** ring is off-resonance with  $\lambda = 1.54 \mu\text{m}$

channel is again almost near 100 % and the peak of resonance yet happens at  $\lambda = 1.576 \mu\text{m}$ . In addition, the full-width-half-maximum (FWHM) bandwidth of filter from  $\lambda = 1.566 \sim 1.583 \mu\text{m}$  is calculated about 17nm which shows a slight increase rather the four-port CDF.

One can find the CW FDTD numerical simulation results of three-port CDF for the wavelength of resonance,  $\lambda = 1.576 \mu\text{m}$  and an arbitrary non-resonant wavelength  $\lambda = 1.54 \mu\text{m}$  in Fig. 7a, b. The electric field component inside the ring resonator again has formed a WG-like mode with azimuthal mode number  $m = 10$ .

### 3.2 Q-factor calculation for all-circular PhC ring resonator

The cavity modes of the studied ring-type PhC are somehow analogous to whispering gallery modes. For a perfectly circular cavity, there is only one non-degenerate monopole mode. Similarly, there is only one monopole for PhC cavities. Analogous to higher order WGMs, PhC WG-like modes are twice degenerate with their modal field patterns shifted by  $(180^\circ/2m)$  with respect to each other, where “ $m$ ” is the WG(-like) azimuthal mode number. Although because of the absence of perfectly circular symmetry in our PhC cavity, these WG-like modes are not exactly degenerate but they form a close doublet which the field pattern of each of these doublets repeats itself by  $(180^\circ/m)$ .

The WG-like modes are calculated using the PWE method with the condition of an appropriate supercell size. Figure 8 shows the PhC ring resonator structure along the chosen supercell which is used to calculate the WG-like modes. We chosen a  $9a \times 9a$  dimension for the supercell and the optimum number of bands that we used to calculate the supercell band structure according to the equation-(1) is found to be  $9 \times (2 + 9) = 99$ . This equation was suggested by Fan et al. (1998) in which the  $x$  and  $y$  are supercell dimensions.

$$Number = [(Min(x, y) + 2) \times (Max(x, y))] \tag{1}$$

Figure 9 shows the field distribution patterns of the main WG-like modes of the all-circular PhC ring resonator. These modes are named M1-M9 respectively and they were calculated using PWE method for the  $|E_y|^2$  electric field component with the TM polarization for  $k = \Gamma$  symmetry point. As we found out from the CW FDTD simulations, the main whispering gallery like mode that resonate in our PhC ring resonator has an azimuthal mode number  $m = 10$ . In Fig. 9, one can see that there is  $18^\circ$  phase shift between corresponding doublets of  $m = 10$  with respect to each other. This mode happens when one excites the ring from

**Fig. 8** Demonstration of the PhC ring resonator and the chosen  $9a \times 9a$  supercell. This supercell is used to calculate the whispering gallery modes of the ring resonator structure

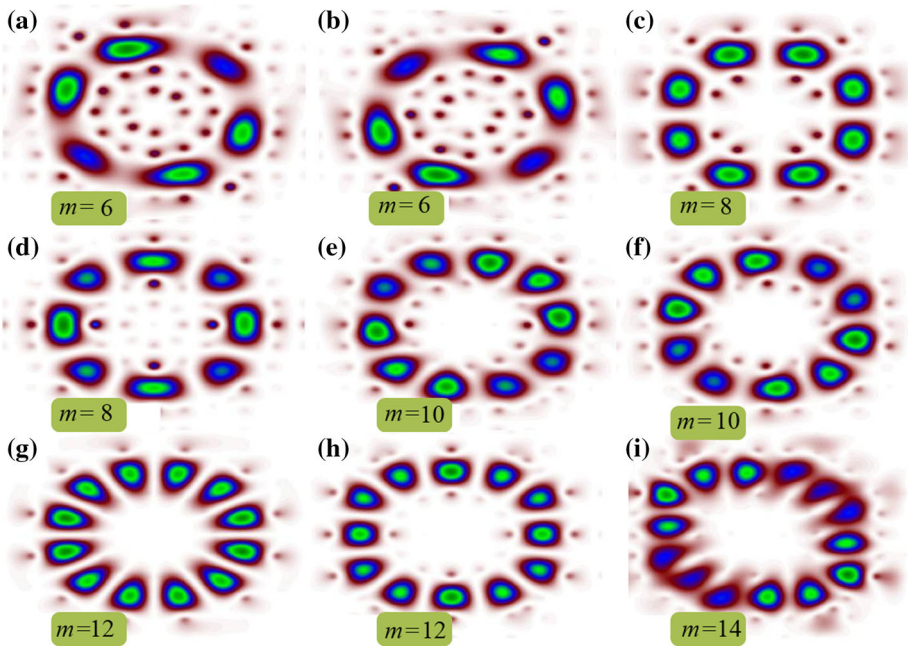
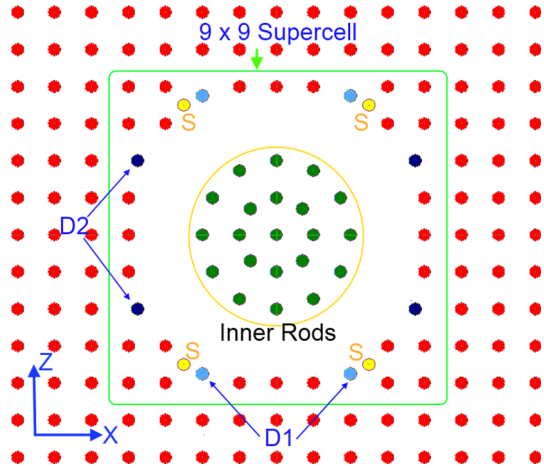


**Fig. 9** The field distribution patterns of the main whispering gallery like modes of the all-circular PhC ring resonator. These modes were calculated using PWE method for the  $|E_y|^2$  electric field component with the TM polarization and for  $k = \Gamma$  symmetry point. In the inset of each plot, the WG-like azimuthal mode numbers are indicated by ‘ $m$ ’

$\Gamma$ - $K$  symmetry point direction. These  $m = 10$  WG-like modes are shown in Fig. 9e, f and their corresponding normalized frequencies are  $a/\lambda = 0.36384$  and  $a/\lambda = 0.36465$ .

Using the FDTD method and employing impulse excitation of the ring resonator in the time domain, the  $Q$ -factors of these M1-M9 modes, their center wavelength and their spectral line width are found which is shown in Table 1 The  $Q$ -factor is calculated as the ratio of  $\lambda_0/\delta\lambda$ . Also the  $Q$ -factors of the doublets of  $m = 10$  are calculated as 1050, and 866 respectively.

**Table 1** The calculated  $Q$ -factors of the M1–M9 whispering gallery like modes with their center wavelength,  $\lambda_0$  and their spectral lines width,  $\delta\lambda$

Mode	$m$	$\lambda_0$ (nm)	$\delta\lambda$ (nm)	$Q$	$\Delta\theta$
M1	6	1,296	2.5	518	30°
M2	6	1,358	4	339	
M3	8	1,438	3.5	410	22.5°
M4	8	1,489	3.5	425	
M5	10	1,560	1.8	866	18°
M6	10	1,575	1.5	1,050	
M7	12	1,657	4	414.25	15°
M8	12	1,690	3.5	483	
M9	14	1,736	5	347.2	–

' $m$ ' is the azimuthal index of WG-like modes and  $\Delta\theta$  denotes the phase shift between their doublets

## 4 Conclusion

In this study, we proposed a four-port and a three-port channel add-drop optical filter based on two-dimensional photonic crystal all circular ring resonators. These structures were made of a square lattice of silicon rods (with the dielectric constant of  $\epsilon_h = 12$ ) surrounded by air and the filling factor of  $r/a = 0.17$ . With the appropriate coupling distance between the PhC ring resonator and bus and drop waveguides, our channel add-drop filter is formed. The dropping efficiency for both filters is close to 100% in their wavelength interval—C (1.535–1.565  $\mu\text{m}$ ) and L (1.565–1.625  $\mu\text{m}$ ) bands of optical telecommunications. We also found that whispering gallery like mode with azimuthal mode number  $m = 10$  resonate in our PhC cavity structure which has a doublet. The normalized frequency of doublets of  $m = 10$  are  $a/\lambda = 0.3684$  and  $0.3645$ ; and their  $Q$ -factors are calculated as 1050, and 866 respectively.

Whispering gallery like modes of the PhC ring resonator and the PhC band structure were calculated using PWE method, hence the  $Q$ -factor of whispering gallery like modes and the transmission spectra of CDFs were calculated using 2D-FDTD numerical method.

## References

- Boriskin, A.V., Boriskina, S.V., Rolland, A., Sauleau, R., Nosich, A.I.: Test of the FDTD accuracy in the analysis of the scattering resonances associated with high-Q whispering-gallery modes of a circular cylinder. *JOSA A* **25**(5), 1169–1173 (2008)
- Bush, K., Lolkes, S., Wehrspohn, R., Foll, H.: *Photonic Crystals*. Wiley, Weinheim (2004)
- Chu, T., Yamada, H., Gomyo, A., Ushida, J., Ishida, S., Arakawa, Y.: Tunable optical notch filter realized by shifting the photonic bandgap in a silicon photonic crystal line-defect waveguide. *IEEE Photonics Technol. Lett.* **18**(24), 2614–2616 (2006)
- Chung, K., Yoon, J.: Properties of a  $1 \times 4$  optical power splitter made of photonic crystal waveguides. *Opt. Quantum Electron.* **35**(10), 959–966 (2003). doi:[10.1023/A:1025173916864](https://doi.org/10.1023/A:1025173916864)
- Djavid, M., Abrishamian, M.S.: Multi-channel drop filters using photonic crystal ring resonators. *Optik—Int. J. Light Electron. Opt.* **123**(2), 167–170 (2012)
- Espinola, R., Ahmad, R., Pizzuto, F., Steel, M., Osgood, R.: A study of high-index-contrast 90 degree waveguide bend structures. *Opt. Express* **8**(9), 517–528 (2001)
- Fan, S., Villeneuve, P.R., Joannopoulos, J.D., Haus, A.: Channel drop filters in photonic crystals. *Opt. Express* **3**, 4–11 (1998)
- Ghadrdan, M., Mansouri-Birjandi, M.A.: Concurrent implementation of all-optical half-adder and AND & XOR logic gates based on nonlinear photonic crystal. *Opt. Quantum Electron.* **45**(10), 1027–1036 (2013)
- Ghaffari, A., Monifi, F., Djavid, M., Abrishamian, M.: Photonic crystal bends and power splitters based on ring resonators. *Opt. Commun.* **281**(23), 5929–5934 (2008a)

- Ghaffari, A., Monifi, F., Djavid, M., Abrishamian, M.S.: Heterostructure wavelength division demultiplexers using photonic crystal ring resonators. *Opt. Commun.* **281**, 4028–4032 (2008b)
- Ghasemi, V.K.H.: Design tunable optical thin film fabry-perot filter in dense wavelength division multiplexer. *Majlesi J. Telecommun. Dev.* **2**(1), 167–171 (2013)
- Gibbs, H.: *Optical Bistability: Controlling Light with Light*. Elsevier, Amsterdam (1985)
- Guo, S., Albin, S.: Numerical techniques for excitation and analysis of defect modes in photonic crystals. *Opt. Express* **11**(9), 1080–1089 (2003)
- Inoue, K., Ohtaka, K.: *Photonic Crystals: Physics, Fabrication and Applications*. Springer, Berlin (2004)
- Janfaza, M., Mansouri-Birjandi, M.A.: Wideband slow light in photonic crystal slab waveguide based on geometry adjustment and optofluidic infiltration. *Appl. Opt.* **52**(34), 8184–8189 (2013)
- Joannopoulos, J., Johnson, S.G., Winn, N., Meade, R.D.: *Photonic Crystal: Molding the flow of light*, 2nd ed. Princeton University Press, Princeton (2008)
- Johnson, S., Joannopoulos, J.: Block-iterative frequency-domain methods for Maxwell's equations in a planewave basis. *Opt. Express* **8**(3), 173–190 (2001)
- Lalanne, P., Mias, S., Hugonin, J.: Two physical mechanisms for boosting the quality factor to cavity volume ratio of photonic crystal microcavities. *Opt. Express* **12**(3), 458–467 (2004)
- Li, J.: Terahertz wave narrow bandpass filter based on photonic crystal. *Opt. Commun.* **283**(13), 2647–2650 (2010)
- Liu, Y., Sarris, C.D.: Fast time-domain simulation of optical waveguide structures with a multilevel dynamically adaptive mesh refinement FDTD approach. *J. Lightwave Technol.* **24**(8), 3235–3247 (2006)
- Manzacca, G., Paciotti, D., Marchese, A., Moreolo, M.S., Cincotti, G.: 2D photonic crystal cavity-based WDM multiplexer. *Photon. Nanostruct. Fundam. Appl.* **5**, 164–170 (2007)
- Meade, R., Rappe, A., Brommer, K., Joannopoulos, J., Alherhand, O.: Erratum: Accurate theoretical analysis of photonic band-gap materials (*Phys. Rev. B* 48, 8434 (1993)). *Phys. Rev.-Sect. B-Condensed Matter* **55**(23), 15942–15943 (1997)
- Monifi, F., Djavid, M., Ghaffari, A., Abrishamian, M.: A new bandstop filter based on photonic crystals. In: *Proceedings of the PIER, Cambridge, USA* (2008)
- Olivier, S., Benisty, H., Smith, C., Rattier, M., Weisbuch, C., Krauss, T.: Transmission properties of two-dimensional photonic crystal channel waveguides. *Opt. Quantum Electron.* **34**(1–3), 171–181 (2002)
- Qiang, Z., Zhou, W., Soref, R.A.: Optical add-drop filters based on photonic crystal ring resonators. *Opt. Express* **15**, 1823–1831 (2007)
- Rafizadeh, D., Zhang, J., Hagness, S., Taflove, A., Stair, K., Ho, S., Tiberio, R.: Waveguide-coupled AlGaAs/GaAs microcavity ring and disk resonators with high finesse and 21.6-nm free spectral range. *Opt. Lett.* **22**(16), 1244–1246 (1997)
- Robinson, S., Nakkeeran, R.: Photonic crystal ring resonator based add-drop filter using hexagonal rods for CWDM systems. *Optoelectron. Lett.* **7**(3), 164–166 (2011)
- Robinson, S., Nakkeeran, R.: PCRR based add drop filter for ITU-T G. 694.2 CWDM systems. *Optik-Int. J. Light Electron Opt.* **124**(5), 393–398 (2013)
- Robinson, S., Nakkeeran, R.: Photonic crystal ring resonator-based add drop filters: a review. *Opt. Eng.* **52**(6), 060901–060901 (2013)
- Saghirzadeh Darki, B., Granpayeh, N.: Improving the performance of a photonic crystal ring-resonator-based channel drop filter using particle swarm optimization method. *Opt. Commun.* **283**(20), 4099–4103 (2010)
- Sakai, A., Baba, T.: FDTD simulation of photonic devices and circuits based on circular and fan-shaped microdisks. *J. Lightwave Technol.* **17**(8), 1493–1499 (1999)
- Sakoda, K.: *Optical Properties of Photonic Crystals*. Springer, Berlin (2005)
- Shlager, K.L., Schneider, J.B.: A selective survey of the finite-difference time-domain literature. *IEEE Antennas Propag. Mag.* **37**(4), 39–57 (1995)
- Stieler, D.P.: *Characterization of Defect Cavities and Channel-Drop Filters in the Three Dimensional Woodpile Photonic Crystal*. Graduate Theses and Dissertations, Iowa State University (2008)
- Stoffer, R., Hoekstra, H., De Ridder, R., Van Groesen, E., Van Beckum, F.: Numerical studies of 2D photonic crystals: waveguides, coupling between waveguides and filters. *Opt. Quantum Electron.* **32**(6–8), 947–961 (2000)
- Suh, W., Fan, S.: All-pass transmission or flat-top reflection filters using a single photonic crystal slab. *Appl. Phys. Lett.* **84**(24), 4905–4907 (2004)
- Tavousi, A., Mansouri-birjandi, M.A., saffari, M.: Add-drop and channel-drop optical filters based on photonic crystal ring resonators. *Int. J. Commun. Inf. Technol.* **2**(1), 19–24 (2012)
- Villeneuve, P.R., Fan, S., Joannopoulos, J.: Microcavities in photonic crystals: mode symmetry, tunability, and coupling efficiency. *Phys. Rev. B* **54**(11), 7837–7842 (1996)
- Vlasov, Y.A., O'Boyle, M., Hamann, H.F., McNab, S.J.: Active control of slow light on a chip with photonic crystal waveguides. *Nature* **438**(7064), 65–69 (2005)

- Xiao, Y.-F., Min, B., Jiang, X., Dong, C.-H., Yang, L.: Coupling whispering-gallery-mode microcavities with modal coupling mechanism. *IEEE J. Quantum Electron.* **44**(11), 1065–1070 (2008)
- Xu, X., Qiang, Z., Jiang, J., Chen, X., Li, H., Qiu, Y.: Modal analysis of ultra-compact channel filters based on race-track photonic crystal ring resonators. *J. Modern Opt.* **58**(11), 932–938 (2011)
- Yariv, A., Yeh, P.: *Photonics: Optical Electronics in Modern Communications* (The Oxford Series in Electrical and Computer Engineering). Oxford University Press Inc., Oxford (2006)
- Yee, K.S.: Numerical solution of initial boundary value problems involving Maxwell's equations. *IEEE Trans. Antennas Propag.* **14**(3), 302–307 (1966)
- Yu, T., He, L., Deng, X., Fang, L., Liu, N.: Power splitter based on photonic crystal waveguides with an air holes array. *Opt. Eng.* **50**(11), 114601 (2011)